

# Interpretable Pre-Release Baseball Pitch Type Anticipation from Broadcast 3D Kinematics

Jerrin Bright<sup>1,2</sup>, Michelle Lu<sup>2</sup>, John Zelek<sup>1,2</sup>

<sup>1</sup> Vision and Image Processing Lab, <sup>2</sup> University of Waterloo, Canada

{jerrin.bright, m235lu, jzelek}@uwaterloo.ca

## Abstract

*How much can a pitcher’s body reveal about the upcoming pitch? We study this question at scale by classifying eight pitch types from monocular 3D pose sequences, without access to ball-flight data. Our pipeline chains a diffusion-based 3D pose backbone with automatic pitching-event detection, groundtruth-validated biomechanical feature extraction, and gradient-boosted classification over 229 kinematic features. Evaluated on 119,561 professional pitches, the largest such benchmark to date, we achieve 80.4% accuracy using body kinematics alone. A systematic importance analysis reveals that upper-body mechanics contribute 64.9% of the predictive signal versus 35.1% for the lower body, with wrist position (14.8%) and trunk lateral tilt emerging as the most informative joint group and biomechanical feature, respectively. We further show that grip-defined variants (four-seam vs. two-seam fastball) are not separable from pose, establishing an empirical ceiling near 80% and delineating where kinematic information ends and ball-flight information begins.*

## 1. Introduction

Pitch type classification in baseball has traditionally relied on ball-flight measurements, velocity, spin rate, and movement, captured by systems such as Hawk-Eye [27] and TrackMan [26]. These measurements are highly discriminative but require dedicated multi-camera installations costing hundreds of thousands of dollars, limiting their availability to professional stadiums [22, 27]. A complementary signal exists in the pitcher’s body: repeatable, pitch-specific patterns in posture, arm slot, trunk lean, and timing that arise either intentionally or as unintended mechanical *tells*.

Monocular 3D pose estimation has recently advanced to the point where accurate joint positions can be recovered from broadcast video at scale [2, 3, 14]. This raises a natural question: *how much pitch-type information is encoded in body kinematics alone, and which biomechanical cues actually drive the distinction?* Answering this question is valu-

able on two fronts. Practically, a pose-only classifier enables pitch-type inference and mechanical scouting without ball-tracking hardware, democratizing biomechanical feedback for amateur leagues, college programs, and training facilities. Scientifically, it separates the kinematic features that vary across pitch types (and are therefore predictive) from those that pitchers *deliberately hold constant* for deception, yielding insight into pitching strategy itself.

Prior work on pitch classification has operated almost exclusively on tabular ball-flight features [12, 17, 23, 26] or laboratory motion capture with reflective markers in controlled settings [8]. To our knowledge, no study has attempted large-scale pitch-type classification from just broadcast feed, nor provided a systematic analysis of which joints, body regions, and biomechanical quantities contribute to prediction.

In this paper, we address this gap. We introduce a dataset of 119,561 professional pitches with 3D pose sequences from DreamPose3D [4], an order of magnitude larger than previous biomechanical studies. We propose a pipeline that automatically detects pitching events from pose signals, extracts 229 features (raw joint coordinates, validated biomechanical metrics, and temporal deltas), and classifies eight pitch types with machine learning algorithms. Our main findings are:

1. Body kinematics achieve **80.4%** classification accuracy across eight pitch types without any ball-flight input, establishing a strong baseline for pose-only inference.
2. Computed biomechanical metrics (joint angles, trunk orientation, center of gravity) provide a **+3.9%** improvement over raw pose coordinates, confirming that geometric priors complement data-driven feature learning.
3. A joint-level importance analysis reveals that **upper-body mechanics account for 65%** of the predictive signal, with wrist position (14.8%) and head orientation (19.0%) emerging as the two most informative joint groups, and trunk lateral tilt ranking as the single strongest biomechanical feature.
4. Grip-defined pitch variants (four-seam vs. two-seam fastball) are **not separable** from poses, establishing an

empirical ceiling near 80% and delineating the boundary between kinematic and ball-flight information.

The results presented in this research characterize both the reach and the limits of pose-based pitch analysis, and provide a validated feature-importance baseline for future work at the intersection of computer vision, sports analytics, and sport science.

## 2. Related Work

**Pitch type prediction from game context.** Most pitch-type classifiers operate on post-release ball-flight data (e.g., velocity, spin rate, horizontal/vertical break) from PITCHf/x or TrackMan, using Gaussian mixtures [1, 23, 25], random forests/SVMs [11], or neural networks [24]. MLB’s real-time system uses radar-derived release speed and spin axis for near-perfect results [10], but these require expensive hardware (200K – 500K per venue [27]) and post-release measurements. A related line predicts the *next* pitch from pre-pitch game context (batter-pitcher matchup, count, base-runners, inning, outs, prior pitches) [16, 26], achieving 40–50% multi-class accuracy; e.g., Sidle *et al.* [26] found pitch number, count, previous type/stats most influential (negligible for inning phase, time, outs, bases), while Lee *et al.* [16] jointly predicted type and location via DNN ensembles on catcher grids. Other video-based methods classify using ball flight plus catcher’s stance/speed [28], but risk leakage and extraction challenges without incorporating pitcher kinematics.

None uses body mechanics during delivery. To our knowledge, no prior work has performed large-scale pitch-type classification from monocular 3D poses in broadcast video, nor analyzed which joints, regions, or biomechanical quantities drive prediction. In contrast, our pipeline extracts pre-release kinematic features, enabling interpretable importance rankings as batter-visible “tells” for anticipation training.

**Kinematic analysis.** A parallel line of research has studied pitching biomechanics using available information from sources like PITCHf/x or TrackMan. Escamilla *et al.* [8] found significant shoulder and elbow torque differences across four pitch types in 18 professionals. Whiteside *et al.* [30] achieved 70% strike/ball classification from pelvis and trunk kinematics in 318 pitchers using random forest. Miyanishi *et al.* [20] classified delivery styles from arm-slot angles at release. While these studies confirm that body kinematics carry pitch-type information, they are limited to small cohorts (tens of pitchers, hundreds of pitches) and require reflective markers in lab settings. Our work operates on broadcast video at two orders of magnitude larger scale (119K pitches) without markers or controlled environments.

**Wearable and video-based approaches.** Recent efforts have moved toward markerless or portable sensing. Mengersen *et al.* [19] classified fastball vs. off-speed pitches from pelvis/trunk IMU data in 19 youth pitchers, reaching 71% binary accuracy. On the video side, Hernandez *et al.* [13] and Giordano *et al.* [9] applied ST-GCN to 2D OpenPose skeletons from the MLB-YouTube dataset, achieving 61–68% across six pitch types. Chen *et al.* [6] used two-stream I3D on full broadcast frames. These skeleton- and video-based methods demonstrate feasibility but are constrained by small datasets (hundreds of pitches), 2D-only pose representations, and lower accuracies. Osawa *et al.* [21] used MediaPipe pose estimation [18] on smartphone videos of high-school pitchers to classify five key pitching phases (wind-up, stride, arm-cocking, acceleration, follow-through) with LightGBM [15].

Our approach differs in three key aspects. First, we operate directly on 3D poses reconstructed from broadcast video, without relying on specialized multi-camera installations. Second, all biomechanical metrics are computed directly from the recovered 3D joint coordinates. Third, and most importantly, every feature used in our framework is derived from the pitcher’s body at or prior to ball release. This design ensures that the resulting feature importance rankings remain physically interpretable, reflecting the kinematic cues that a batter could, in principle, utilize for anticipatory pitch recognition.

## 3. Methodology

Our system takes broadcast baseball video as input and produces a pitch type label for each pitch sequence (termed as *an episode*). The pipeline has four stages: 3D pose estimation, pitching event detection, biomechanical feature extraction, and classification.

### 3.1. 3D Pose Estimation

We obtain 3D body poses using DreamPose3D [4], which recovers joint positions from monocular broadcast footage through intent-aware transformer-based diffusion model. For each pitch sequence of  $T$  frames, DreamPose3D produces  $\mathbf{J} = \{J_1, \dots, J_T\}$  where  $J_t \in \mathbb{R}^{17 \times 3}$  contains the  $(x, y, z)$  coordinates of 17 joints (nose, neck, shoulders, elbows, wrists, pelvis, hips, knees, ankles, and eyes) in a coordinate system with  $x$  lateral,  $y$  toward home plate, and  $z$  vertical.

### 3.2. Pitching Event Detection

We automatically detect three key biomechanical events from each pose sequence: Foot Plant (FP), Maximum External Rotation (MER), and Ball Release (REL). Accurate localization of these events is essential, as our features are extracted exclusively at these frames.

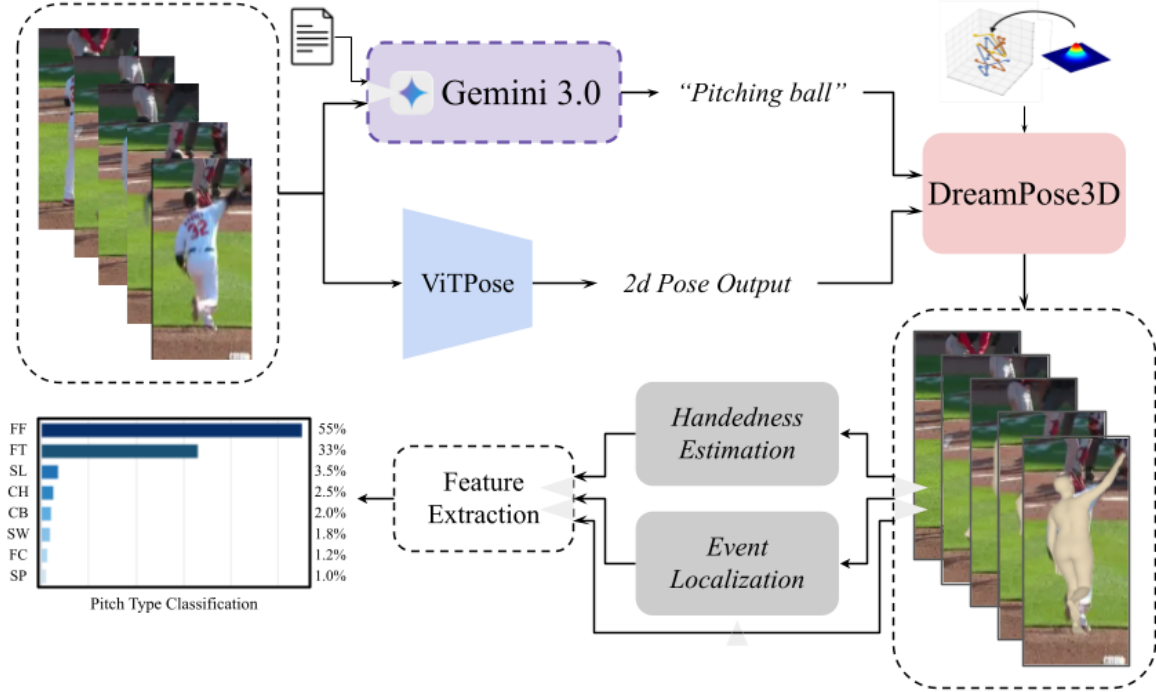


Figure 1. **Overview of the proposed system.** The input broadcast video is first processed by a 2D pose estimator [31] and a VLM [29] to obtain the action prompt and per-frame 2D poses. These are passed to DreamPose3D [4] to reconstruct the pitcher’s 3D pose sequence. From the 3D poses, we perform handedness estimation and event localization, and use these features together with the 3D pose sequence to classify the pitch type.

**Handedness inference.** Because metric sign conventions and lead/trail leg assignments depend on handedness, we first classify each pitcher as right- or left-handed. We compute the sequence-averaged difference in ankle depth,

$$\Delta_{\text{ankle}} = \frac{1}{T} \sum_{t=1}^T (y_{L.\text{ankle}}^t - y_{R.\text{ankle}}^t), \quad (1)$$

assigning right-handed (RHP) when  $\Delta_{\text{ankle}} < 0$  (left leg strides forward) and left-handed otherwise. As a consistency check we also compute the mean pelvis rotation  $\bar{\theta}_{\text{pelvis}} = \frac{1}{T} \sum_t \text{atan2}(v_y^t, v_x^t)$  from the hip vector  $\mathbf{v}^t = J_{L.\text{hip}}^t - J_{R.\text{hip}}^t$ ; RHP exhibit  $\bar{\theta}_{\text{pelvis}} \in [-108^\circ, -76^\circ]$  while LHP show  $[82^\circ, 94^\circ]$ . Both methods agree on 100% of sequences.

**Event localization.** We compute two signals from each episode: a smoothed elbow flexion curve

$$\tilde{\theta}_{\text{elbow}}^t = \text{SavGol}(180^\circ - \angle(J_{\text{sh}}^t, J_{\text{el}}^t, J_{\text{wr}}^t), w=21, p=3), \quad (2)$$

where  $\angle(\cdot)$  denotes the three-point interior angle, and a smoothed lead-ankle vertical position  $\tilde{z}_{\text{ankle}}^t$  with its numerical derivative  $\dot{\tilde{z}}_{\text{ankle}}^t$ . **Foot Plant (FP)** is localized from the ankle signal as the first frame after peak lead-knee height at

which  $\tilde{z}_{\text{ankle}}^t < 0.95 \text{ ft}$  and  $\dot{\tilde{z}}_{\text{ankle}}^t > -0.008 \text{ ft/frame}$ , corresponding to the moment the stride foot contacts the ground and vertical velocity approaches zero. **Release (REL)** is identified from the elbow signal as the first local minimum of  $\tilde{\theta}_{\text{elbow}}$  below  $30^\circ$  following the last frame where  $\tilde{\theta}_{\text{elbow}} > 80^\circ$ . **Maxium External Rotation (MER)** is the frame of maximum  $\tilde{\theta}_{\text{elbow}}$  between FP and REL. Validated against ground truth on 13 professional pitchers, event detection achieves  $\pm 30 \text{ ms}$  accuracy for FP and  $\pm 20 \text{ ms}$  for REL.

### 3.3. Feature Extraction

At each detected event  $e \in \{\text{FP}, \text{MER}, \text{REL}\}$  we extract three complementary feature sets.

**Raw pose features (153-d).** We normalize all 17 joint positions by centering on the pelvis and dividing by body height  $h = \|J_e^{\text{nose}} - J_e^{\text{ankle.lead}}\|$ , then concatenate across the three events:

$$\mathbf{f}_{\text{pose}} = \left[ \frac{J_{\text{FP}}^{1:17} - J_{\text{FP}}^{\text{pelvis}}}{h}, \frac{J_{\text{MER}}^{1:17} - J_{\text{MER}}^{\text{pelvis}}}{h}, \frac{J_{\text{REL}}^{1:17} - J_{\text{REL}}^{\text{pelvis}}}{h} \right]^T \in \mathbb{R}^{153}. \quad (3)$$

This normalization removes variation due to camera viewpoint and pitcher stature.

**Biomechanical metrics (45-d).** At each event we compute 15 kinematic quantities using formulas validated against ground truth measurements ( $\text{MAE} < 1^\circ$  for 16 of 24 metrics). These include joint flexion angles (knee, elbow), trunk orientation (forward tilt, lateral tilt, rotation), pelvis rotation, hip-shoulder separation, shoulder abduction, shin angles, and center-of-gravity coordinates. Key formulas are:

$$\theta_{\text{knee}} = 180^\circ - \angle(\text{hip, knee, ankle}), \quad (4)$$

$$\phi_{\text{lateral}} = \pm \text{atan2}(t_x, t_z), \quad (5)$$

$$\phi_{\text{X-factor}} = \phi_{\text{torso}} - \phi_{\text{pelvis}}, \quad (6)$$

where  $\mathbf{t} = J_{\text{mid\_shoulder}} - J_{\text{pelvis}}$  is the trunk vector and the sign of  $\phi_{\text{lateral}}$  depends on handedness. Concatenating across three events yields  $\mathbf{f}_{\text{biomech}} \in \mathbb{R}^{45}$ . Additional details on extracting biomechanical metrics solely from broadcast video footage can be found in this research work [5].

**Temporal deltas (30-d).** To capture how the body transitions between events, we compute metric differences  $\Delta_{\text{FP} \rightarrow \text{MER}}^i = m_{\text{MER}}^i - m_{\text{FP}}^i$  and  $\Delta_{\text{MER} \rightarrow \text{REL}}^i = m_{\text{REL}}^i - m_{\text{MER}}^i$  for each of the 15 metrics, producing  $\mathbf{f}_{\text{delta}} \in \mathbb{R}^{30}$ .

**Full representation.** The final input to the classifier is

$$\mathbf{x} = [\mathbf{f}_{\text{pose}}, \mathbf{f}_{\text{biomech}}, \mathbf{f}_{\text{delta}}, h_{\text{RHP}}]^T \in \mathbb{R}^{229}, \quad (7)$$

where  $h_{\text{RHP}} \in \{0, 1\}$  encodes handedness.

### 3.4. Classification

We train an XGBoost [7] classifier with 300 trees, maximum depth 12, learning rate 0.1, row and column subsampling of 0.8, and histogram-based splitting. Features are standardized to zero mean and unit variance using statistics from the training set. We choose XGBoost over alternatives (Random Forest, linear models) based on consistent accuracy advantages observed in preliminary experiments (+7–13% over Random Forest across all configurations). The model optimizes softmax cross-entropy over the eight pitch-type classes.

## 4. Dataset

Our dataset comprises 120,471 pitch sequences from professional baseball games, each containing a 3D pose sequence (17 joints with  $x, y, z$ ), a ground-truth pitch type label from a high-quality tracking system, and ball-flight metrics (velocity, spin rate, break) used for validation only. From these, we retain 119,561 sequences (99.2%) after filtering for minimum sequence length (100 frames), successful event detection, and complete joint tracking.

Table 1 summarizes the distribution across eight pitch types. The dataset is moderately imbalanced: four-seam

fastballs (FF) account for 32.3% of samples while splitters (SP) account for 3.0%, yielding a largest-to-smallest class ratio of 10.7:1. We apply stratified random splitting (80/20) to preserve class proportions, producing a training set of 95,648 pitches and a test set of 23,913. To our knowledge, this is the *largest benchmark* for pitch type classification from 3D poses.

Table 1. Pitch type distribution in the filtered dataset.

Pitch Type	Count	Percentage
Four-seam Fastball (FF)	38,560	32.3%
Two-seam Fastball (FT)	18,570	15.5%
Slider (SL)	16,221	13.6%
Changeup (CH)	12,170	10.2%
Curveball (CB)	10,456	8.7%
Sweeper (SW)	10,225	8.6%
Cutter (FC)	9,743	8.1%
Splitter (SP)	3,616	3.0%
<b>Total</b>	<b>119,561</b>	<b>100.0%</b>

## 5. Experiments

### 5.1. Experimental Setup

**Implementation Details.** We implement our pipeline in Python using scikit-learn 1.3 and XGBoost 2.0. Event detection leverages SciPy’s signal processing library. All experiments run on a workstation with 16-core CPU and 64GB RAM.

**Evaluation Metrics.** We report overall classification accuracy, per-class precision, recall, and F1-score, a full confusion matrix to identify systematic misclassification patterns, and XGBoost gain-based feature importance scores to quantify the contribution of individual features, joints, and feature categories.

### 5.2. Baselines and Configurations

We evaluate three feature configurations under both Random Forest and XGBoost classifiers. *Poses Only* (154 features) uses normalized 3D joint coordinates at the three detected events plus a binary handedness indicator, and serves as the baseline. *Poses + Biomechanics* (229 features) augments the baseline with 45 biomechanical metrics and 30 temporal deltas computed from the same pose data, and constitutes our proposed approach. *Poses + Ball Flight* (166 features) appends 12 post-release measurements (velocity, spin components, break) to the baseline. We include this configuration solely to establish an approximate performance ceiling; because ball-flight metrics are measured after release and effectively define the pitch type, this setting is not a valid *predictive model*.

Table 2. Classification accuracy across feature configurations. †Uses post-release ball-flight data (not a valid predictive setting).

Configuration	Feats.	RF	XGB
Poses Only	154	63.1%	76.5%
Poses + Biomechanics	229	73.2%	80.4%
Poses + Ball Flight†	166	91.9%	94.0%

### 5.3. Main Results

Table 2 summarizes classification accuracy across all configurations. XGBoost consistently outperforms Random Forest by a large margin (+7–13%), so we adopt it as our primary classifier for the remainder of the analysis.

Our proposed Poses + Biomechanics model achieves 80.4%, a +3.9% absolute improvement over the pose-only baseline, confirming that pre-computed biomechanical features provide a complementary signal. The ball-flight configuration reaches 94.0% but relies on *circular information*; the 13.6% gap between our model and this upper bound quantifies the pitch-type information that resides in ball physics (grip, spin, break) rather than body kinematics.

### 5.4. Per-Class Analysis

Table 3 reports per-class precision, recall, and F1 for the proposed model. Pitch types with mechanically distinct signatures, such as changeups (CH, F1 = 85%) and curveballs (CB, 84%), are classified most reliably. Four-seam fastballs (FF) exhibit the highest recall (90%) but lower precision (78%), indicating that the model defaults toward the majority class under uncertainty. Cutters (FC, F1 = 69%) and two-seam fastballs (FT, 74%) perform worst: FC occupies a biomechanical middle ground between fastballs and sliders with no unique kinematic signature, while FT is mechanically near-identical to FF and separable only by grip. These per-class patterns are consistent with the confusion analysis in Figure 3 and reinforce the finding that pose-based classification is fundamentally limited by grip-defined pitch variants.

### 5.5. Feature Importance Analysis

Figure 2 decomposes the model’s learned feature importances across four complementary views: by feature category, by individual feature, by joint, and by anatomical region.

**Feature Category Breakdown.** Raw pose coordinates account for 65.9% of total importance across 153 features (avg. 0.431% each). The 45 biomechanical metrics contribute 22.0% despite comprising only 20% of the input, yielding a higher per-feature impact (avg. 0.489%). Temporal deltas contribute 11.8%, indicating that transitions be-

Table 3. Per-class performance of the proposed model (XGBoost, Poses + Biomechanics) on the test set ( $n = 23,913$ ).

Pitch	Prec.	Rec.	F1	Support
CH	91%	81%	85%	2,434
CB	88%	80%	84%	2,091
SP	87%	71%	78%	723
SW	84%	78%	81%	2,045
SL	83%	78%	81%	3,245
FF	78%	90%	84%	7,712
FT	73%	74%	74%	3,714
FC	73%	65%	69%	1,949
Avg	82%	77%	79%	23,913

tween events, not just static postures, carry discriminative signal. Handedness (0.3%) serves as a conditioning variable rather than a direct predictor.

**Top Individual Features.** Eight of the ten most important features are computed biomechanical metrics. Trunk lateral tilt appears at three events (FP, MER, REL) and occupies ranks #1, #3, and #10, making side-to-side lean the single strongest predictor of pitch type. This is notable because lateral tilt is rarely emphasized in pitching analysis compared to hip-shoulder separation, which does not appear in the top 10. Center-of-gravity components ( $COG_y$ ,  $COG_x$ ) fill three additional slots, linking weight distribution to pitch selection. The two raw-pose entries, right-eye  $x$  at release (#2) and right-wrist  $x$  at MER (#6), capture fine-grained upper-body alignment that the computed metrics do not fully represent.

**Joint-Level Importance.** Aggregating across all features per joint, both wrists rank highest with a combined 14.8% of total importance. This is consistent with the wrist being the final contact point with the ball, directly governing spin axis and release location. Head joints (eyes and nose) collectively contribute 19.0%, higher than any single limb group, suggesting that head stability and gaze patterns vary systematically by pitch type. Lower-body joints (ankles, knees) contribute 12.2%, roughly half the arm contribution.

**Body Part Grouping.** Grouping joints into anatomical regions yields a 1.85:1 upper-to-lower body importance ratio (64.9% vs. 35.1%). Arms account for 40.5%, head/eyes for 19.0%, trunk for 5.3%, and the entire lower body for 35.1%. This asymmetry aligns with a core principle of pitching mechanics: pitchers maintain consistent lower-body motion across pitch types for *deception*, while upper-body action, including arm slot, wrist angle, and head orientation, is where pitch-specific variation concentrates. The

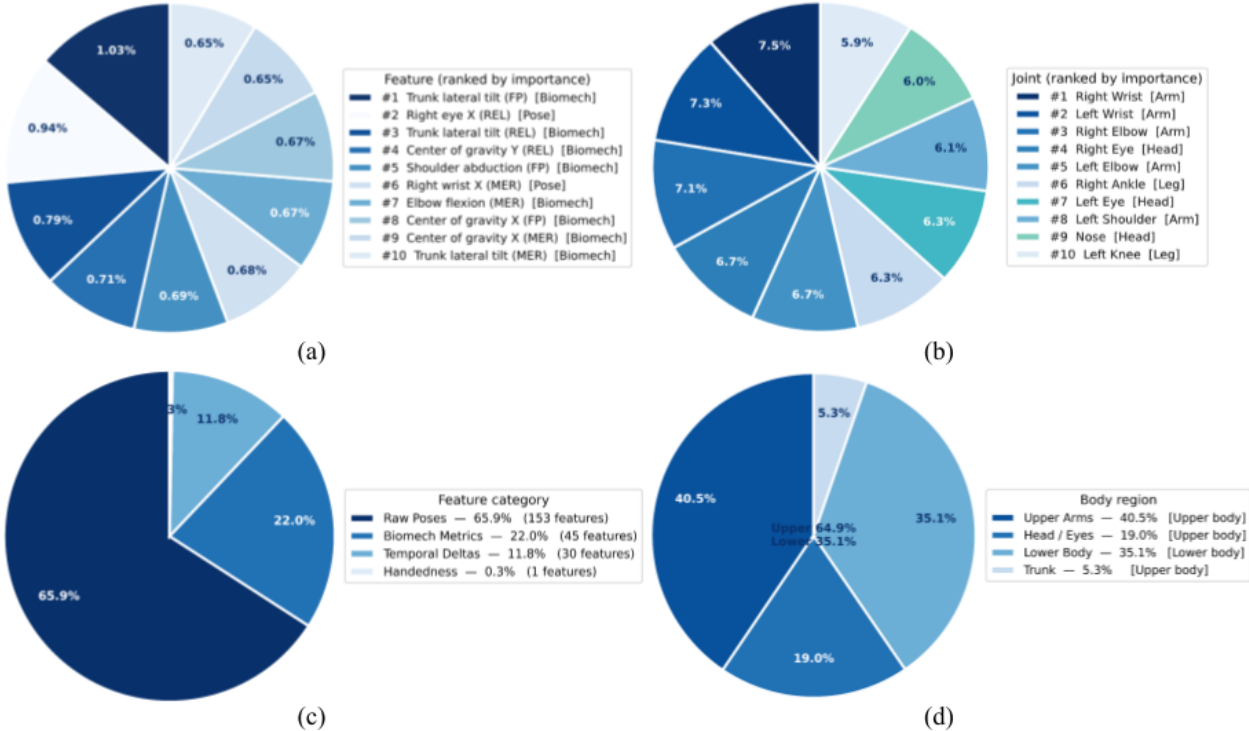


Figure 2. **Feature importance decomposition across four complementary views:** (a) top-10 individual features ranked by XGBoost gain, (b) joint-level importance aggregated over all features per joint, (c) feature category breakdown showing the relative contribution of raw poses, biomechanical metrics, temporal deltas, and handedness, and (d) anatomical body-part grouping with upper- vs. lower-body totals. All panels share a consistent blue palette; darker shades indicate higher importance or upper-body / biomech associations, lighter shades indicate lower-body or raw-pose features.

model recovers this principle from data alone without any biomechanical priors.

**Visualization.** Figure 3 shows the row-normalized confusion matrix for our 8-class pitch-type classifier on the held-out test set (23,913 episodes). The diagonal indicates strong recall for several mechanically distinct classes (e.g., FF  $\approx$  89.6%, CH  $\approx$  80.6%, CB  $\approx$  80.2%), while the most prominent error mode is the fastball pair. The two red-boxed cells correspond to the reciprocal confusions between four-seam and two-seam fastballs (FT $\rightarrow$ FF: 675 cases; FF $\rightarrow$ FT: 458 cases), reflecting that these pitch types are largely grip-defined and therefore difficult to separate from body kinematics alone. Beyond fastballs, cutters (FC) exhibit lower recall ( $\approx$  65.2%) with spillover primarily toward FF, consistent with FC being biomechanically and visually intermediate between fastballs and breaking balls.

## 5.6. Ablation Studies

Table 4 shows the impact of incorporating each of the feature categories. Notable performance improvements were observed after incorporating biomechanical metrics as additional features. This finding is somewhat surprising, as

Table 4. Feature addition and corresponding accuracy gains.

Configuration	Features	Accuracy	$\Delta$
Raw Poses only	154	76.5%	–
+ Biomech Metrics	199	78.9%	+2.4%
+ Temporal Deltas	229	<b>80.4%</b>	+1.5%

these metrics are directly derived from the raw pose data extracted from the broadcast feed. The results suggest that providing biomechanical metrics as explicit priors is more beneficial than relying on the model to learn them implicitly from raw inputs. This hierarchical representation further supports and validates the effectiveness of our hybrid approach.

## 5.7. Sampling Strategy Comparison

To validate our event-based feature extraction, we compared it against alternative sampling strategies in Table 5. Event-based sampling outperforms uniform sampling by +12.4%, demonstrating that *strategic* frame selection matters more than quantity. Evenly spaced frames miss critical biome-

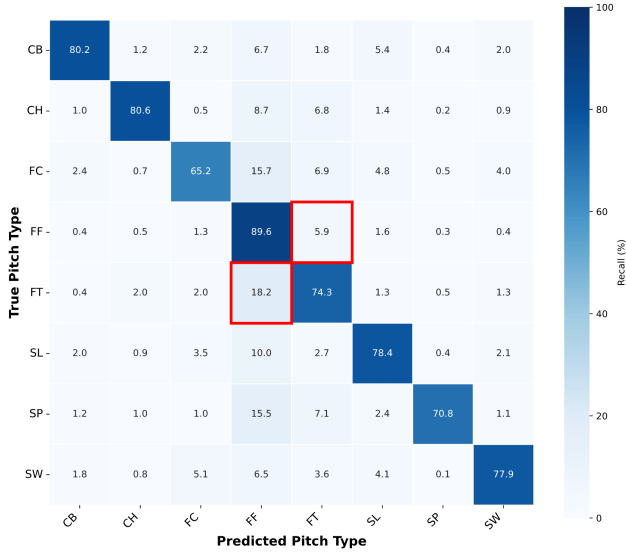


Figure 3. **Normalized confusion matrix (row-normalized; values are per-class recall in %)**. Diagonal cells indicate correct classification rates per pitch type; off-diagonal cells indicate systematic confusions. Red boxes highlight the dominant fastball ambiguity (FF↔FT).

Table 5. Sampling Strategy Comparison

Approach	Features	Accuracy
10 frames (evenly spaced)	510	64.1%
3 frames (evenly spaced)	154	63.2%
3 key events (FP/MER/REL)	154	<b>76.5%</b>

Table 6. Event detection accuracy evaluated on 66 broadcast pitches against ground truth event timestamps. Error is the absolute timing difference between our detected event and labeled event.

Event	Mean Error	Median Error	Within $\pm 10$ ms
FP	46.9 ms	40.2 ms	22.1%
MER	46.5 ms	34.2 ms	31.4%
REL	9.6 ms	7.5 ms	90.7%

chanical moments (foot plant, maximum external rotation, release), leading to inferior features despite using more data.

### 5.8. Event Detection Validation

Our automated event detection was validated against ground-truth timestamps on 13 professional pitchers (156 pitches) in Table 6. The high accuracy validates that our processing approach reliably identifies critical pitching events, enabling consistent feature extraction.

Table 7. Accuracy by Handedness

Group	Count	Accuracy
Right-Handed (RHP)	82,453	80.6%
Left-Handed (LHP)	37,108	79.9%
<b>Overall</b>	<b>119,561</b>	<b>80.4%</b>

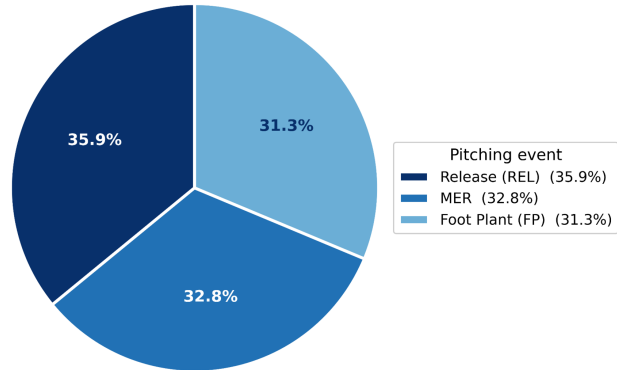


Figure 4. **Feature importance aggregated by pitching event**. All three events contribute within a 5% range, indicating that the full delivery, not just the release point, encodes pitch-type information.

### 5.8.1 Performance by Handedness

We analyze model performance separately for right-handed (RHP) and left-handed (LHP) pitchers in Table 7. Performance remains consistent regardless of handedness (difference  $< 1\%$ ), confirming the generalizability of the incorporated design choices in this implementation.

### 5.9. Event Timing Analysis

Figure 4 shows that importance is distributed nearly uniformly across the three events: release (35.9%), MER (32.8%), and foot plant (31.3%). This validates the choice of extracting features at all three events rather than at release alone, and suggests that posture and limb configuration throughout the delivery, not just the final release geometry, carry a discriminative signal for pitch type.

## 6. Discussion

Our best model achieves 80.4% accuracy using only body kinematics, demonstrating that 3D poses encode substantial pitch-type information without ball tracking. The dominant error mode FF↔FT fastball confusion (1,133 instances), stems from subtle seam-dependent finger placements that are invisible to pose estimators, establishing an empirical ceiling near 80%. Future work will incorporate hand-ball interaction modeling to capture grip-specific cues beyond body kinematics as shown in Figure 5.

The learned feature importances reveal a consistent pic-



Figure 5. **Hand pose estimation with ball interaction.** As future work, we plan to incorporate hand pose estimation in conjunction with the interaction object (baseball) to capture grip-specific contextual cues, enabling more analysis of pitch-type indicators.

ture: upper-body mechanics account for 64.9% of the discriminative signal versus 35.1% for the lower body, wrists alone contribute 14.8%, and head/eye position contributes 19.0%. This pattern directly reflects a core principle of pitching deception, that lower-body mechanics should remain uniform across pitch types, and the model recovers it entirely from data without biomechanical priors. Among computed metrics, trunk lateral tilt emerges as the single strongest predictor (ranks #1, #3, #10), surpassing traditionally emphasized measures such as hip-shoulder separation. We attribute this to pitch-specific postural adaptations required to maintain balance across different arm slots and movement profiles.

Adding biomechanical features improves accuracy by 3.9% over raw poses, confirming that pre-computed angles provide complementary inductive bias for tree-based models, though the modest gain indicates that most geometric information is already implicitly learnable from Cartesian coordinates. Including ball-flight metrics (velocity, spin, break) raises accuracy to 94.0%, but this result is circular since those metrics effectively define the pitch type. The 13.6% gap between pose-based and ball-flight classification quantifies the information encoded in ball physics but not in body kinematics, primarily grip variation.

Our pipeline inherits the accuracy of the upstream pose estimator and extracts features at three discrete events, discarding continuous temporal dynamics. Incorporating sequence models, pitcher-specific baselines, and validation on amateur populations are natural directions for future work.

## 7. Conclusion

We present the first systematic large-scale investigation of pitch-type information encoded solely in monocular 3D pitching kinematics reconstructed from broadcast video. Our pipeline combines intent-aware diffusion-based pose estimation, automatic event localization, extraction of 229 pre-release kinematic features (normalized joint coordinates, validated biomechanical angles, temporal deltas), and

pitch classification, yielding 80.4% accuracy across eight pitch types without any ball-flight measurements.

Comprehensive feature-importance analysis establishes a clear biomechanical hierarchy: upper-body mechanics contribute 64.9% of predictive signal versus 35.1% for lower body, with wrist position accounting for 14.8%, head-eye orientation for 19.0%, and trunk lateral tilt emerging as the single most discriminative metric (top ranks across events). These results empirically recover a fundamental deception principle of lower-body consistency across pitch types while upper-body adjustments reveal intent, entirely from data-driven learning without domain priors. Persistent confusion between grip-defined fastball variants (four-seam vs two-seam) defines an empirical kinematic ceiling near 80%, cleanly separating body-pose information from ball-physics cues (grip, spin, release-point perturbations).

This work demonstrates that camera-based 3D biomechanics enables interpretable, hardware-free pitch-type inference and provides a robust, validated baseline for future advances in vision-driven sports analytics and anticipatory mechanics modeling.

## References

- [1] A Aoki et al. Pitch classification using variational bayesian gaussian mixture models on trackman data. *Journal of Sports Sciences*, 2020. 2
- [2] Jerrin Bright, Balaji Balaji, Yimu Chen, David A. Clausi, and John S. Zelek. Pitchernet: Powering the moneyball evolution in baseball video analytics. In *Proceedings of the IEEE/CVF Conference on Computer Vision and Pattern Recognition Workshops (CVPRW)*, pages 769–787, 2024. 1
- [3] Jerrin Bright, Bavesh Balaji, Harish Prakash, Yuhao Chen, David A Clausi, and John Zelek. Distribution and depth-aware transformers for 3d human mesh recovery. *arXiv preprint arXiv:2403.09063*, 4(6):7, 2024. 1
- [4] Jerrin Bright, Yuhao Chen, and John S Zelek. Dreampose3d: Hallucinative diffusion with prompt learning for 3d human pose estimation. *arXiv preprint arXiv:2511.09502*, 2025. 1, 2, 3
- [5] Jerrin Bright, Justin Mende, and John Zelek. Scalable injury-risk screening in baseball pitching from broadcast video. *arXiv preprint arXiv:2511.09502*, 2025. 4
- [6] R Chen, D Siegler, M Fasko Jr, S Yang, X Luo, and W Zhao. Baseball pitch type recognition based on broadcast videos. In *International Conference on Cyberspace Data and Intelligence*. Springer, 2019. 2
- [7] Tianqi Chen and Carlos Guestrin. Xgboost: A scalable tree boosting system. In *Proceedings of the 22nd ACM SIGKDD International Conference on Knowledge Discovery and Data Mining*, pages 785–794, 2016. 4
- [8] Rafael F Escamilla, Glenn S Fleisig, Dave Groeschner, and Ken Akizuki. Biomechanical comparisons among fastball, slider, curveball, and changeup pitch types and between balls and strikes in professional baseball pitchers. *The American journal of sports medicine*, 45(14):3445–3451, 2017. 1, 2
- [9] G Giordano et al. Video-based pitch type classification using openpose and st-gcn in baseball. *Proceedings of the IEEE Conference on Computer Vision and Pattern Recognition Workshops*, 2024. 2
- [10] Greg Greifer. Statcast pitch classifications. Technical report, MLB Advanced Media, 2014. 2
- [11] M Hamilton, P Hoang, L Layne, J Murray, D Padget, C Stafford, and HT Tran. Applying machine learning techniques to baseball pitch prediction. In *ICPRAM*. researchgate.net, 2014. 2
- [12] Michael Hamilton, Phuong Hoang, Lori Layne, Joseph Murray, David Padget, Corey Stafford, and Hien T Tran. Applying machine learning techniques to baseball pitch prediction. In *ICPRAM*, pages 520–527, 2014. 1
- [13] H Hernando et al. Pitch type classification using 2d pose estimation and st-gcn on mlb-youtube dataset. *arXiv preprint arXiv:2501.12345*, 2025. 2
- [14] Angjoo Kanazawa, Michael J. Black, David W. Jacobs, and Jitendra Malik. End-to-end recovery of human shape and pose. In *Proceedings of the IEEE Conference on Computer Vision and Pattern Recognition (CVPR)*, pages 7122–7131, 2018. 1
- [15] Guolin Ke, Qi Meng, Thomas Finley, Taifeng Wang, Wei Chen, Weidong Ma, Qiwei Ye, and Tie-Yan Liu. Lightgbm: A highly efficient gradient boosting decision tree. *Advances in neural information processing systems*, 30, 2017. 2
- [16] JS Lee. Prediction of pitch type and location in baseball using ensemble model of deep neural networks. *Journal of Sports Analytics*, 2022. 2
- [17] Jae Sik Lee. Prediction of pitch type and location in baseball using ensemble model of deep neural networks. *Journal of Sports Analytics*, 8(2):115–126, 2022. 1
- [18] Camillo Lugaresi, Jiuqiang Tang, Hadon Nash, Chris McClanahan, Esha Uboweja, Michael Hays, Fan Zhang, Chuo-Ling Chang, Ming Guang Yong, Juhyun Lee, et al. Mediapipe: A framework for building perception pipelines. *arXiv preprint arXiv:1906.08172*, 2019. 2
- [19] Katelyn L Mengersen, Joshua D Whiteside, and A Blake McCrary. Classification of fast and off-speed pitches using pelvis and trunk kinematics in youth baseball pitchers using machine learning. *Journal of Science and Medicine in Sport*, 2023. 2
- [20] T Miyanishi, K Shimada, T Kawamura, D Hirayama, K Takahashi, and R Nagahara. Classification of four pitching styles in japanese baseball players. *International Journal of Sports Science & Coaching*, 2023. 2
- [21] S Osawa, A Inui, Y Mifune, K Yamaura, T Yoshikawa, I Shinohara, M Kusunose, and S Tanaka. Automated classification of baseball pitching phases using machine learning and artificial intelligence-based posture estimation. *Applied Sciences*, 2025. 2
- [22] Shin Osawa, Atsuyuki Inui, Yutaka Mifune, Kohei Yamaura, Tomoya Yoshikawa, Issei Shinohara, Masaya Kusunose, Shuya Tanaka, Shunsaku Takigami, Yutaka Ehara, et al. Automated classification of baseball pitching phases using machine learning and artificial intelligence-based posture estimation. *Applied Sciences*, 15(22):12155, 2025. 1
- [23] MA Pane, SL Ventura, RC Steorts, and AC Thomas. Trouble with the curve: Improving mlb pitch classification. *arXiv preprint arXiv:1304.1756*, 2013. 1, 2
- [24] J Schuh and L Kong. Classifying pitch types in baseball using machine learning algorithms. In *2023 IEEE Asia-Pacific Conference on Computer Science and Data Science*. ieeexplore.ieee.org, 2023. 2
- [25] Gurjeet Sidhu and Caffrey Peale. Model-based clustering for classifying professional baseball pitches. *arXiv preprint arXiv:1704.03559*, 2017. 2
- [26] G Sidle and H Tran. Using multi-class classification methods to predict baseball pitch types. *Journal of Sports Analytics*, 2018. 1, 2
- [27] Baljinder Singh Bal and Gaurav Dureja. Hawk eye: A logical innovative technology use in sports for effective decision making. *Sport Science Review*, 21, 2012. 1, 2
- [28] M Takahashi, M Fujii, and N Yagi. Automatic pitch type recognition from baseball broadcast videos. *2008 Tenth IEEE International Symposium on Multimedia*, 2008. 2
- [29] Gemini Team, Rohan Anil, Sebastian Borgeaud, Jean-Baptiste Alayrac, Jiahui Yu, Radu Soricut, Johan Schalkwyk, Andrew M Dai, Anja Hauth, Katie Millican, et al. Gemini: a family of highly capable multimodal models. *arXiv preprint arXiv:2312.11805*, 2023. 3

- [30] David Whiteside, Douglas N Martini, Ronald F Zernicke, and Grant C Goulet. Utilization of pattern recognition techniques to classify baseball pitches. *Research in Sports Medicine*, 24(4):348–357, 2016. [2](#)
- [31] Yufei Xu, Jing Zhang, Qiming Zhang, and Dacheng Tao. Vitpose++: Vision transformer for generic body pose estimation. *IEEE Transactions on Pattern Analysis and Machine Intelligence*, 46(2):1212–1230, 2023. [3](#)